24th INTERNATIONAL CONGRESS ON SOUND AND VIBRATION
23–27 July 2017, London

COMPARISON OF MICROPHONE ARRAY GEOMETRIES FOR MULTI-POINT SOUND FIELD REPRODUCTION

Philip Coleman, Miguel Blanco Galindo, Philip J. B. Jackson
Centre for Vision, Speech and Signal Processing, University of Surrey, Guildford, GU2 7XH, UK
email: p.d.coleman@surrey.ac.uk

Multi-point approaches for sound field control generally sample the listening zone(s) with pressure microphones, and use these measurements as an input for an optimisation cost function. A number of techniques are based on this concept, for single-zone (e.g. least-squares pressure matching (PM), brightness control, planarity panning) and multi-zone (e.g. PM, acoustic contrast control, planarity control) reproduction. Accurate performance predictions are obtained when distinct microphone positions are employed for setup versus evaluation. While, in simulation, one can afford a dense sampling of virtual microphones, it is desirable in practice to have a microphone array which can be positioned once in each zone to measure the setup transfer functions between each loudspeaker and that zone. In this contribution, we present simulation results over a fixed dense set of evaluation points comparing the performance of several multi-point optimisation approaches for 2D reproduction with a 60 channel circular loudspeaker arrangement. Various regular setup microphone arrays are used to calculate the sound zone filters: circular grid, circular, dual-circular, and spherical arrays, each with different numbers of microphones. Furthermore, the effect of a rigid spherical baffle is studied for the circular and spherical arrangements. The results of this comparative study show how the directivity and effective frequency range of multi-point optimisation techniques depend on the microphone array used to sample the zones. In general, microphone arrays with dense spacing around the boundary give better angular discrimination, leading to more accurate directional sound reproduction, while those distributed around the whole zone enable more accurate prediction of the reproduced target sound pressure level.

Keywords: sound zones, microphone arrays

1. Introduction

Personal sound zones aim to deliver audio content to individual listeners sharing the same acoustic space, such as a living room or car, removing the need for them to wear headphones [1, 2]. They have the potential to allow content producers to deliver increasingly personalised experiences to their audience. A number of methods to deliver personal sound zones have been proposed, including analytical methods [3, 4], and multi-point methods based on pressure matching [5, 6, 7, 8] and energy maximisation [9, 10, 11]. When there is a single listener, or multiple listeners listening to the same audio (with no requirement to produce a cancellation region), a similar set of approaches can be applied [12, 13, 14]. Among these methods, multi-point optimisation approaches have proven to be popular for practical applications [15, 16, 17] as the transfer responses from the loudspeakers to a set of control points can easily be measured.

However, in the literature, the design of the control points is typically not considered as a variable for experiments. Some considerations have been given to frequency-dependent zone sampling (to avoid ill conditioning in the system) [18] and ensuring sufficiently dense sampling of the zone [19].

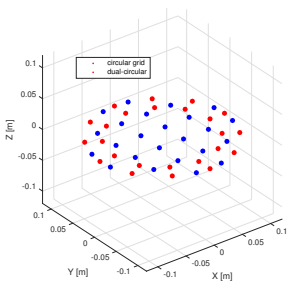

(a) Grid (2.5, 4.0, 6.2 kHz)
Dual-circular (1.6, 3.0, 6.0 kHz)

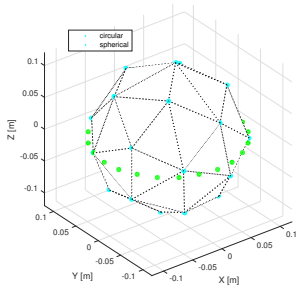

(b) Circular (3.0, 6.0, 12.0 kHz)
Spherical (1.4, 2.0, 2.8 kHz)

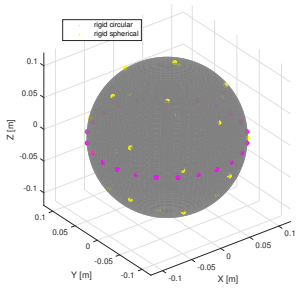

(c) Rigid circular (2.7, 5.7, 12.0 kHz)
Rigid spherical (1.3, 1.9, 2.8 kHz)

Figure 1: Microphone array geometries (illustrating $M = 24$ microphones), including the spatial aliasing limits (kHz) for (12, 24, 48) microphones.

On the other hand, it would be useful in practical applications to be able to place a single microphone array in each zone to conduct in-situ measurements. This would minimise the measurement effort and allow rapid prototyping and evaluation of reproduction systems, and could potentially be used by retailers to perform calibration in a customer's own listening room.

In this paper, we investigate arrangements of control points for multi-point optimisation based on a number of classical microphone array geometries, with feasible numbers of microphones for a single device. The arrays are introduced in Sec. 2, the optimisation methods and experiment setup are described in Sec. 3, the results are presented in Sec. 4, and the findings are discussed in Sec. 5.

2. Microphone arrays

Four microphone array geometries were tested: grid, circular, dual-circular, and spherical. In addition, the circular and spherical baffles were tested with a rigid spherical baffle, giving six test cases in total. Each array was designed to sample a zone with radius $r = 0.11$ m. For each array geometry, $M = \{12, 24, 48\}$ microphones were tested. The array geometries are illustrated in Fig. 1. Microphones in the grid array were arranged to fall within the bounds of a circle with the zone radius. For the open arrays, transfer functions to each microphone were calculated in the frequency domain based on the path length d from a sound source, $e^{-jkd}/4\pi d$. In the presence of the rigid baffle, the transfer functions were calculated in the frequency domain based on a spherical harmonic description of the pressure on the surface of the sphere, following [20].

As the microphone array geometries under test have fixed aperture and number of sensors, the arrangement of microphones results in significant differences in the spatial resolution of the arrays, which may affect their suitability for reproducing directional sound fields. The upper spatial aliasing limits for each array geometry are indicated in the captions of Fig. 1. For fixed M, the circular arrays give the smallest inter-element spacing and thus the highest spatial aliasing limit. Conversely, the spherical arrays distribute the elements widely and give the lowest spatial aliasing limits. The arrays under test allow us to investigate whether it is more useful, with a single zone measurement and a fixed number of microphones, to have dense sampling around the zone boundary, or to cover the zone evenly.

3. Experiments

3.1 Evaluation procedure

For each microphone array, a common reproduction geometry was utilised, comprising a circular array of 60 loudspeakers around a radius of 1.68 m, surrounding two zones. The zones were defined to have radius $r = 0.11$ m, and had 1 m between the zone centres. The geometry is identical to [21] apart

Table 1: Multi-point optimisation cost functions to calculate source weights $\mathbf{q}$ for the methods under test, together with the key references. For a single frequency, $\mathbf{p}_A$ and $\mathbf{p}_B$ are the vectors of complex pressures in zones A (target) and B, $\mathbf{Y}_A$ is a steering matrix relating the zone A microphones to the local angular spectrum, $\mathbf{\Gamma}$ is a diagonal matrix to apply directional weighting to the optimisation, $\mathbf{d}_A$ is the vector of desired target zone pressures, μ and λ are Lagrange multipliers, A and Q denote target sound pressure level and source weight norm, and $\Phi_p\{\}$ denotes the principal eigenvector of a matrix.

	Cost Function	Solution
PP [14]	$\max \mathbf{p}_A^H \mathbf{Y}_A^H \mathbf{\Gamma} \mathbf{Y}_A \mathbf{p}_A - \lambda(\mathbf{q}^H\mathbf{q} - Q)$	$\mathbf{q} \propto \Phi_p\{\mathbf{G}_A^H \mathbf{Y}_A^H \mathbf{\Gamma} \mathbf{Y}_A \mathbf{G}_A\}$
PM-1 [22]	$\min \lvert\lvert\mathbf{p}_A - \mathbf{d}_A\rvert\rvert_2^2 + \lambda(\mathbf{q}^H\mathbf{q} - Q)$	$\mathbf{q} = (\mathbf{G}_A^H\mathbf{G}_A + \lambda\mathbf{I})^{-1}\mathbf{G}_A^H\mathbf{d}_A$
ACC [9]	$\min \mathbf{p}_B^H\mathbf{p}_B + \mu(\mathbf{p}_A^H\mathbf{p}_A - A) + \lambda(\mathbf{q}^H\mathbf{q} - Q)$	$\mathbf{q} \propto \Phi_p\{(\mathbf{G}_B^H\mathbf{G}_B + \lambda\mathbf{I})^{-1}(\mathbf{G}_A^H\mathbf{G}_A)\}$
PC [11]	$\min \mathbf{p}_B^H\mathbf{p}_B + \mu(\mathbf{p}_A^H\mathbf{Y}_A^H\mathbf{\Gamma}\mathbf{Y}_A\mathbf{p}_A - A) + \lambda(\mathbf{q}^H\mathbf{q} - Q)$	$\mathbf{q} \propto \Phi_p\{(\mathbf{G}_B^H\mathbf{G}_B + \lambda\mathbf{I})^{-1}(\mathbf{G}_A^H\mathbf{Y}_A^H\mathbf{\Gamma}\mathbf{Y}_A\mathbf{G}_A)\}$
PM-2 [5]	$\min \mathbf{p}_B^H\mathbf{p}_B + \lvert\lvert\mathbf{p}_A - \mathbf{d}_A\rvert\rvert_2^2 + \lambda(\mathbf{q}^H\mathbf{q} - Q)$	$\mathbf{q} = (\mathbf{G}^H\mathbf{G} + \lambda\mathbf{I})^{-1}\mathbf{G}^H\mathbf{d}$

from the zone spacing, which is slightly narrower here. A common evaluation grid was used for each microphone array under test, having spacing of 2 cm within a circular boundary, giving a total of 101 microphones. The observed pressures in the zones, $\mathbf{o}_A$ and $\mathbf{o}_B$, were used to calculate the evaluation metrics of acoustic contrast (AC), array effort (AE), planarity (η), sound pressure level (SPL) error (ϵ_{SPL}), and direction of arrival (DOA) error (ϵ_{DOA}). AC (dB), AE (dB) and η (%) demonstrate the key features of sound zone system performance [2] and were calculated following [21], ϵ_{SPL} quantifies the variation in SPL (dB) over frequency, which is related to the target zone frequency response, and ϵ_{DOA} quantifies the difference (in degrees) between the direction of the reproduced plane wave energy arriving at the zone and the target direction. The latter metrics were calculated as root-mean-square errors compared to the reference values. The loudspeaker array and evaluation grid were on the same horizontal plane. Source weights and evaluation metrics were calculated in the frequency domain with 50 Hz sampling between 100 Hz and 8 kHz.

3.2 Multi-point optimisation methods

Five multi-point optimisation methods were included in the tests. For directional single-listener reproduction, planarity panning (PP) [14] and pressure matching (PM-1) [22] were used; for multi-zone reproduction, acoustic contrast control (ACC) [9], planarity control (PC) [11], and pressure matching (PM-2) [5] were tested. The cost functions and solutions are collated in Table 1. The implementations follow [21]. The methods are based on sampling the sound field in the zones with the pressure microphone arrays under test, giving vectors of pressures $\mathbf{p}_A$ and $\mathbf{p}_B$ of dimensions $(1 \times M)$. For each method, a target SPL of 76 dB was set for the bright zone. The regularisation constraint was set, for each frequency, to ensure that the array effort did not exceed 0 dB, having first increased the diagonal loading parameter such that the matrix condition number did not exceed 10^{10}. The steering matrices $\mathbf{Y}_A$ of dimensions $(M \times 360)$ were set by superdirective beamforming with one degree angular resolution, following [23], with frequency-independent regularisation of $\beta = 0.01$ for each microphone array geometry. For PP and PC, the target incoming energy direction was set (via the diagonal of $\mathbf{\Gamma}$) to arrive from zero degrees (top to bottom), as in [21]. The PM target fields were set to correspond to a plane wave propagating from zero degrees, and the dark zone pressure for PM-2 was set to zero (i.e., no zone weighting was applied). For the spherical microphone arrays, the PM weights were set independent of the vertical displacement, i.e., the impinging plane wave was assumed to be due to a line source.

Table 2: Summary performance for single zone reproduction (PP and PM-1), for each microphone array geometry with 48 microphones, in terms of array effort (AE), planarity (η), target sound pressure level deviation (ϵ_{SPL}), and target target energy direction error (ϵ_{DOA}) averaged over 200–6000 Hz.

	PP				PM-1			
	AE	η	ϵ_{SPL}	ϵ_{DOA}	AE	η	ϵ_{SPL}	ϵ_{DOA}
Grid	-10.2	89.8	0.0	5.9	-0.7	91.9	0.0	0.0
Circ	-9.6	89.5	0.1	4.5	-2.5	91.7	0.1	0.0
D-circ	-9.7	90.7	0.0	4.9	-2.2	92.3	0.0	0.0
Sph	-9.9	90.2	0.0	5.2	-0.7	92.1	0.0	0.0
RCirc	-10.8	91.7	1.6	3.9	-4.4	57.3	1.3	0.0
RSph	-10.8	90.6	1.4	4.2	-1.8	76.4	1.2	0.2

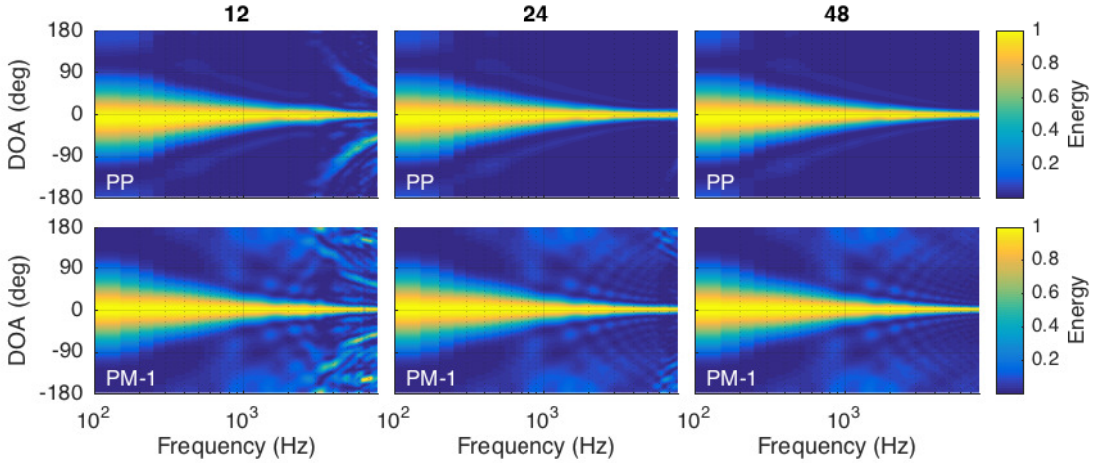

Figure 2: Single zone performance comparing different numbers of microphones for the rigid circular array, showing PP and PM-1.

4. Results

The performance of each of the microphone arrays for the single zone case with 48 microphones is shown in Table 2, with the log-weighted frequency average over 200–6000 Hz stated in each case. For these methods, the array design does not make a significant difference to the performance. The rigid baffled arrays tend to give the lowest array effort, but conversely they give the highest variation from the target SPL value over frequency. On the other hand, the open arrays allow the optimisation better to predict the eventual SPL. The dual-circular array gives a consistently high planarity for both PP and PM-1, suggesting that it is able well to discriminate among energy arriving from different directions. For PP, the rigid circular array gives a slightly higher planarity than the dual-circular array, and the lowest DOA error among the microphone arrays tested. On the other hand, the presence of the rigid baffles for PM-1 significantly degrades the resultant planarity. This effect is particularly pronounced at higher frequencies where the reproduction wavelength becomes comparable to the size of the rigid baffle, and the PM-1 optimisation incorporates amplitude differences due to the baffle that are removed in evaluation.

An example of the reproduced single zone directivity is shown in Fig. 2, for the rigid circular array, for 12, 24, and 48 microphones. For both PP and PM, the energy is placed at the correct position, and the beam widths are similar for both methods. The figure illustrates the effects caused by calculating PM-1 source weights in the presence of a baffle and then removing it for evaluation. In particular, from about 800 Hz, some sound energy begins to impinge from directions other than the target of zero degrees. The corresponding energy patterns are consistent with changing M, meaning that the effect is caused by the size of the baffle itself. In addition, the effects of spatial aliasing can be seen

Table 3: Summary performance for multi-zone reproduction (ACC, PC, and PM-2), for each microphone array, in terms of acoustic contrast (AC), array effort (AE), planarity (η), target sound pressure level deviation (ϵ_{SPL}), and target target energy direction error (ϵ_{DOA}) averaged over 200–6000 Hz.

	ACC				PC					PM-2				
	AC	AE	η	ϵ_{SPL}	AC	AE	η	ϵ_{SPL}	ϵ_{DOA}	AC	AE	η	ϵ_{SPL}	ϵ_{DOA}
Grid	73.8	-12.0	17.7	0.2	71.6	-8.9	87.9	0.1	6.2	51.5	-0.4	91.1	0.0	0.4
Circ	75.3	-11.3	19.4	1.2	75.9	-8.5	86.9	0.4	6.2	54.1	-0.6	88.0	0.1	0.1
D-circ	73.5	-11.5	23.1	0.7	69.7	-8.6	88.1	0.3	5.4	54.9	-0.6	91.7	0.0	0.2
Sph	75.9	-11.6	22.1	0.3	75.7	-8.7	87.7	0.1	6.6	53.3	-0.4	91.2	0.0	0.3
RCirc	72.7	-11.8	24.3	3.6	73.9	-9.7	88.5	1.8	5.4	57.2	-2.1	56.9	1.4	0.1
RSph	74.6	-11.9	25.2	1.8	74.5	-9.8	87.5	1.4	7.2	50.3	-1.8	76.7	1.2	0.4

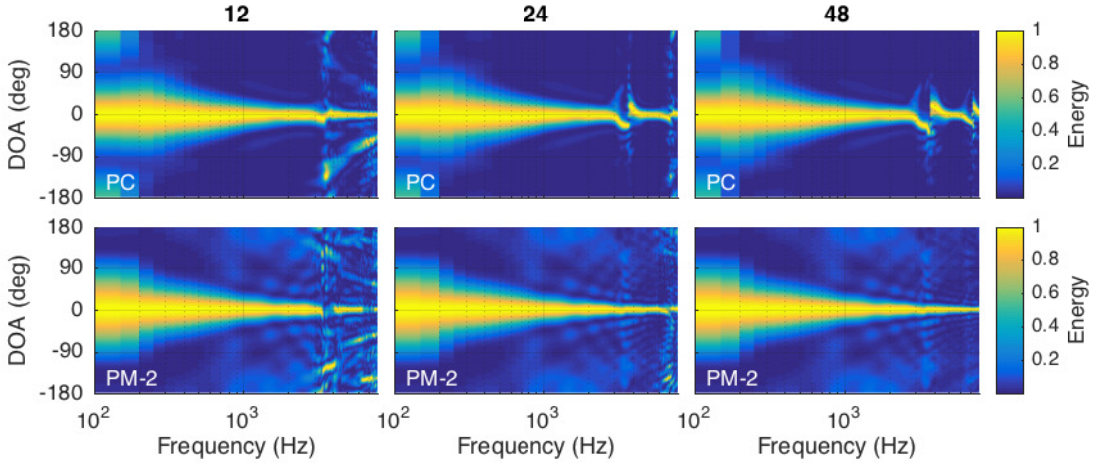

Figure 3: Multi-zone performance comparing different numbers of microphones for the rigid circular array, showing PC and PM-2.

for the 12 and 24 microphone cases, and PM-1 seems to be more sensitive than PP in terms of energy impinging from directions outside the target DOA.

An overview of the results for the multi-zone case with 48 microphones is shown in Table 3 (log-weighted frequency averages over 200–6000 Hz). The DOA error is not included for ACC as there is no reference in this case. For ACC and PC, the best AC values are achieved with the open spherical and circular arrays, although, as for the single zone case, the open circular array gives the least consistent target zone SPL among the open arrays. As for the single zone case, the grid and open spherical arrays give the least variation in SPL, for all methods, while the rigid arrays introduce problems in this regard. In general, the trends for multi-zone PC follow those for single zone PP, and similarly, the trends are similar between PM-2 and PM-1. In essence, the dual-circular and rigid circular arrays give the highest planarity and lowest DOA error for PC, while the performance under these metrics falls away for PM-2 for the rigid circular array, compared to the dual-circular. The directivity for the multi-zone case with the rigid circular array with different numbers of microphones is shown in Fig. 3. Similar to Fig. 2, for the single zone case, it can be seen that the presence of the rigid baffle spreads the range of DOAs for PM-2 more than those for PC. In addition to the spatial limitations of the microphone array itself, discussed above, the plots in Fig. 3 also contain artefacts due to the aliasing behaviour of the loudspeaker array, which has to control a larger region for the multi-zone reproduction. In particular, the deviation from the target DOA observed in PC between 3–4 kHz is due to the loudspeaker array aliasing rather than the microphone array design.

To further illustrate the comparative performance for the multi-zone case, the AC, planarity, and SPL are shown over frequency in Fig. 4, for 48 microphones. In general, a few trends can be seen. The AC values for ACC and PC are not generally affected by the microphone array design beneath

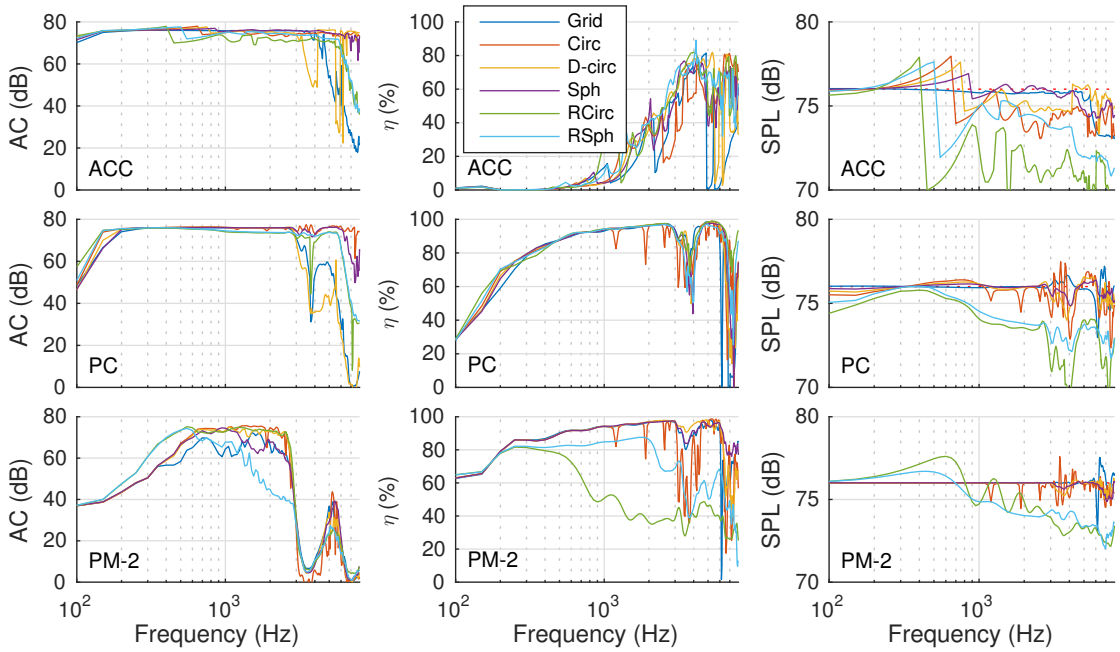

Figure 4: Multi-zone performance comparing microphone arrays under the metrics of acoustic contrast (AC), planarity (η), and target sound pressure level (SPL).

the loudspeaker aliasing limit. However, above this limit, the open circular and spherical arrays maintain high AC, while the other arrays suffer from some performance loss. The dual-circular and grid arrays tend to degrade most, which helps to explain the averaged values in Table 3. The PM-2 performance, on the other hand, is more variable below the loudspeaker array aliasing limit. In particular, the baffled arrays demonstrate an increase in low frequency AC, while the rigid spherical array AC begins to degrade above 1 kHz. As discussed above, the PM-2 planarity drops for the baffled arrays, but the other arrays have generally comparable planarity for PC and PM-2, apart from the open circular array planarity, which exhibits sharp dips across frequency. In terms of the spatially averaged SPL, the open spherical array and grid array tend to give the most even values across frequency, while the SPL for the rigid arrays tends to be lower than the target value. The effect on multi-zone AC when reducing the number of control microphones is shown in Fig. 5 for PC and PM-2 (ACC performance was very similar to PC). The main effect here is to reduce the upper frequency at which AC can be properly created. Consequently, the (open and rigid) circular arrays, with the highest spatial aliasing frequencies, give the best AC performance when the number of microphones is reduced. Furthermore, the role of the baffle in increasing low frequency AC is shown to be maintained when the number of microphones is reduced.

5. Discussion

Six microphone array designs (grid, open circular, dual circular, open spherical, rigid circular and rigid spherical), with 12, 24, or 48 microphones, were investigated to be used as measurement devices for multi-point optimisation-based sound field control. In summary, the results showed that the microphone array design has some effect on the resultant control performance, especially if relatively few microphones are used for multi-zone reproduction. In general, the microphone array geometry made the most difference to the planarity score and the DOA accuracy, with the dual-circular and rigid circular arrays performing strongly. The rigid baffles improved performance at low frequencies. Using a rigid baffle for control microphones and removing it for evaluation led to a low control effort, but accordingly, the target SPL was usually not reached, especially at higher frequencies. The planarity was also affected by this, especially for PM. On the other hand, distributing the microphones

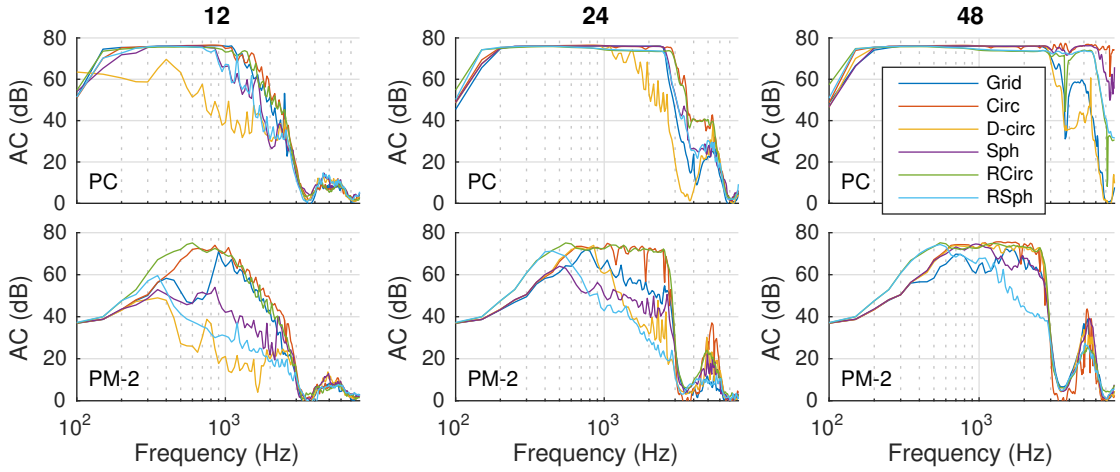

Figure 5: Multi-zone acoustic contrast performance comparing microphone arrays with different numbers of microphones

across the zone led to the most uniform SPL over frequency, but made the AC sensitive in the loudspeaker array aliasing regions. On average, the open spherical array performed quite well for all five multi-point optimisation methods and under all metrics.

Furthermore, a robustness study was conducted by applying various perturbations to the acoustic transfer functions between calculating the source weights and evaluating the resultant performance. Three kinds of errors were introduced: microphone position errors (for example due to manufacturing tolerance) of up to 2 mm and 5 mm, loudspeaker position error of up to 10 mm, and a change in the estimated speed of sound of up to 10 m/s. These experiments showed the main conclusions from the simulations under ideal conditions, presented above, to hold under the tested non-ideal conditions. For single zone reproduction, the presence of errors in the transfer functions did not significantly affect the performance, with the main differences between metrics being due to the optimisation method. In general, the baffled arrays, where the zone SPL predicted during filter calculation is increased by the scattered sound, produce weaker fields in reproduction (with corresponding lower AE), and require equalisation for a flat frequency response. Interestingly, the presence of microphone errors applied to the dual-circular array appeared to improve in terms of AC and planarity, perhaps due to the errors leading to a better conditioned system. The dual-circular array consistently performed well in terms of planarity, in the presence of errors.

Factors for further investigation include the beamformer robustness (used for PP and PC) achieved when applying the same method and regularisation to very different microphone arrays and the effects of varying the desired angle of incidence for the target zone energy.

6. Acknowledgements

This work was supported by the EPSRC Programme Grant S3A: Future Spatial Audio for an Immersive Listener Experience at Home (EP/L000539/1) and the BBC as part of the BBC Audio Research Partnership.

REFERENCES

1. Betlehem, T., Zhang, W., Poletti, M., Abhayapala, T. D., et al. Personal sound zones: Delivering interface-free audio to multiple listeners, *Signal Processing Magazine, IEEE*, **32** (2), 81–91, (2015).
2. Coleman, P., Jackson, P. J. B., Olik, M., Møller, M., Olsen, M. and Pedersen, J. A. Acoustic contrast, planarity and robustness of sound zone methods using a circular loudspeaker array, *The Journal of the Acoustical Society of America*, **135** (4), (2014).

3. Wu, Y. and Abhayapala, T. Spatial multizone soundfield reproduction: Theory and design, *IEEE Transactions on Audio, Speech and Language Processing*, **19** (6), 1711–1720, (2011).
4. Zhang, W., Abhayapala, T. D., Betlehem, T. and Fazi, F. M. Analysis and control of multi-zone sound field reproduction using modal-domain approach, *The Journal of the Acoustical Society of America*, **140** (3), 2134–2144, (2016).
5. Poletti, M. An investigation of 2-D multizone surround sound systems, *Proceedings of the 125th Audio Engineering Society Convention, San Francisco, CA, 2-5 October*, 10, (2008).
6. Simón Gálvez, M. F., Elliott, S. J. and Cheer, J. A superdirective array of phase shift sources, *The Journal of the Acoustical Society of America*, **132** (2), 746–756, (2012).
7. Chang, J.-H. and Jacobsen, F. Sound field control with a circular double-layer array of loudspeakers, *The Journal of the Acoustical Society of America*, **131** (6), 4518–4525, (2012).
8. Radmanesh, N., Burnett, I. S. and Rao, B. D. A lasso-ls optimization with a frequency variable dictionary in a multizone sound system, *IEEE/ACM Transactions on Audio, Speech and Language Processing (TASLP)*, **24** (3), 583–593, (2016).
9. Choi, J.-W. and Kim, Y.-H. Generation of an acoustically bright zone with an illuminated region using multiple sources, *The Journal of the Acoustical Society of America*, **111** (4), 1695–1700, (2002).
10. Shin, M., Lee, S. Q., Fazi, F. M., Nelson, P. A., Kim, D., Wang., S., Park, K. H. and Seo, J. Maximization of acoustic energy difference between two spaces, *The Journal of the Acoustical Society of America*, **128** (1), 121–131, (2010).
11. Coleman, P., Jackson, P. J. B., Olik, M. and Pedersen, J. A. Personal audio with a planar bright zone, *The Journal of the Acoustical Society of America*, **136** (4), 1725–1735, (2014).
12. Ward, D. B. and Abhayapala, T. Reproduction of a plane-wave sound field using an array of loudspeakers, *IEEE Transactions on Speech and Audio Processing*, **9** (6), 697 –707, (2001).
13. Poletti, M. and Betlehem, T. Creation of a single sound field for multiple listeners, *Proc. Internoise*, vol. 249, pp. 2033–2040, Institute of Noise Control Engineering, (2014).
14. Coleman, P. and Jackson, P. J. B. Planarity panning for listener-centered spatial audio, *Audio Engineering Society Conference 55th International Conference on Spatial Audio*, Audio Engineering Society, (2014).
15. Cheer, J., Elliott, S. J., Kim, Y. and Choi, J.-W. Practical implementation of personal audio in a mobile device, *Journal of the Audio Engineering Society*, **61** (5), 290–300, (2013).
16. Cheer, J., Elliott, S. J. and Simón Gálvez, M. F. Design and implementation of a car cabin personal audio system, *Journal of the Audio Engineering Society*, **61** (6), 412–424, (2013).
17. Baykaner, K., Coleman, P., Mason, R., Jackson, P. J., Francombe, J., Olik, M. and Bech, S. The relationship between target quality and interference in sound zone, *Journal of the Audio Engineering Society*, **63** (1/2), 78–89, (2015).
18. Olivieri, F., Fazi, F. M., Shin, M. and Nelson, P. Pressure-matching beamforming method for loudspeaker arrays with frequency dependent selection of control points, *Audio Engineering Society Convention 138*, Audio Engineering Society, (2015).
19. Møller, M. B. and Olsen, M. Sound zones: On performance prediction of contrast control methods, *Audio Engineering Society Conference: 2016 AES International Conference on Sound Field Control*, Audio Engineering Society, (2016).
20. Jarrett, D., Habets, E., Thomas, M. and Naylor, P. Rigid sphere room impulse response simulation: Algorithm and applications, *The Journal of the Acoustical Society of America*, **132** (3), 1462–1472, (2012).
21. Coleman, P. and Jackson, P. Planarity-based sound field optimization for multi-listener spatial audio, *Audio Engineering Society Conference: 2016 AES International Conference on Sound Field Control*, Audio Engineering Society, (2016).
22. Kirkeby, O. and Nelson, P. A. Reproduction of plane wave sound fields, *The Journal of the Acoustical Society of America*, **94** (5), 2992–3000, (1993).
23. Jackson, P. J. B., Jacobsen, F., Coleman, P. and Pedersen, J. A. Sound field planarity characterized by superdirective beamforming, *Proceedings of Meetings on Acoustics*, vol. 19, p. 055056, Montreal, 2-7 June 2013, (2013).